

Improving the orbital-free density functional theory description of covalent materials

Baojing Zhou

Department of Chemistry and Biochemistry, University of California, Los Angeles, Los Angeles, California 90095-1569

Vincent L. Ligneres

Department of Chemistry and Biochemistry, University of California, Los Angeles, Los Angeles, California 90095-1569 and Department of Chemistry, Princeton University, Princeton, New Jersey 08544

Emily A. Carter

Department of Chemistry and Biochemistry, University of California, Los Angeles, Los Angeles, California 90095-1569 and Department of Mechanical and Aerospace Engineering and Program in Applied and Computational Mathematics, Princeton University, Princeton, New Jersey 08544

(Received 28 September 2004; accepted 26 October 2004; published online 4 January 2005)

The essential challenge in orbital-free density functional theory (OF-DFT) is to construct accurate kinetic energy density functionals (KEDFs) with general applicability (i.e., transferability). During the last decade, several linear-response (LR)-based KEDFs have been proposed. Among them, the Wang-Govind-Carter (WGC) KEDF, containing a density-dependent response kernel, is one of the most accurate that still affords a linear scaling algorithm. For nearly-free-electron-like metals such as Al and its alloys, OF-DFT employing the WGC KEDF produces bulk properties in good agreement with orbital-based Kohn-Sham (KS) DFT predictions. However, when OF-DFT, using the WGC KEDF combined with a recently proposed bulk-derived local pseudopotential (BLPS), was applied to semiconducting and metallic phases of Si, problems arose with convergence of the self-consistent density and energy, leading to poor results. Here we provide evidence that the convergence problem is very likely caused by the use of a truncated Taylor series expansion of the WGC response kernel. Moreover, we show that a defect in the ansatz for the first-order reduced density matrix underlying the LR KEDFs limits the accuracy of these KEDFs. By optimizing the two free parameters involved in the WGC KEDF, the two-body Fermi wave vector mixing parameter γ and the reference density ρ_* used in the Taylor expansion, OF-DFT calculations with the BLPS can achieve semiquantitative results for nine phases of bulk silicon. These new parameters are recommended whenever the WGC KEDF is used to study nonmetallic systems. © 2005 American Institute of Physics. [DOI: 10.1063/1.1834563]

I. INTRODUCTION

Among all the first-principles methods based on density functional theory (DFT),¹ the linear scaling orbital-free (OF)-DFT scheme may be the most capable of treating large systems (> 1000 atoms) at lowest cost.²⁻⁴ Unlike traditional orbital-based first-principles techniques, such as Hartree-Fock⁵ and Kohn-Sham (KS)-DFT,⁶ the OF-DFT method avoids solving self-consistently for one-electron orbitals and instead only utilizes the electron density, a function of three coordinates, as its sole variational parameter.⁷ Consequently, the costs associated with manipulating orbitals (e.g., orthonormalization) are completely eliminated. For periodic systems, the advantage of using OF-DFT is even more remarkable, since no k -point sampling is necessary, leading to many orders of magnitude savings for metallic systems, in particular.

Although the earliest OF-DFT, namely, the Thomas-Fermi (TF) model,⁸ appeared much earlier before today's widely used KS-DFT, OF-DFT has not become a mainstream quantum mechanics method for practical applications. The

main obstacle lies in the lack of accurate kinetic energy density functionals (KEDFs) that can be evaluated with linear scaling algorithms. If this stumbling block could be removed, then one could fully exploit the power of the original Hohenberg-Kohn theorems.¹ Namely, one could calculate the ground state density, and other properties not explicitly dependent on the many-body wave function, by directly minimizing the following total electronic energy functional with respect to the electron density ρ :

$$E_v[\rho] = T_s[\rho] + E_H[\rho] + E_{xc}[\rho] + \int \rho(\mathbf{r})v(\mathbf{r})d\mathbf{r}, \quad (1)$$

under the constraint that ρ is properly normalized to N , the number of electrons in the system. Here v is the external potential (typically, the electron-nuclear attraction term), T_s is the kinetic energy of a noninteracting system of electrons whose density is the same as the interacting electron system, E_H is the classical Hartree repulsion energy, and E_{xc} is the exchange-correlation energy (E_{xc} also includes the differ-

ence between the interacting and noninteracting kinetic energies). This naturally leads to the Thomas-Fermi-Hohenberg-Kohn (TFHK) equation

$$\frac{\delta E_v[\rho]}{\delta \rho(\mathbf{r})} = \frac{\delta T_s[\rho]}{\delta \rho(\mathbf{r})} + \frac{\delta E_H[\rho]}{\delta \rho(\mathbf{r})} + \frac{\delta E_{xc}[\rho]}{\delta \rho(\mathbf{r})} + v(\mathbf{r}) = \mu, \quad (2)$$

where μ is the Lagrange multiplier that guarantees the correct normalization of the electron density during the minimization and corresponds to the chemical potential after the total energy $E_v[\rho]$ is minimized.

In addition to the KEDF problem, another challenge for OF-DFT applied to condensed matter is the need for a smooth yet accurate potential⁹ to represent the interaction of the valence electrons with the core electrons and the nuclei. In KS-DFT, this problem is often circumvented by using high quality nonlocal pseudopotentials (NLPSs).^{10,11} Unfortunately, NLPSs utilize projections onto orbitals and therefore cannot be used in OF-DFT. Recently, a new scheme was developed by us to generate transferable LPSs derived from bulk crystalline densities.¹² We showed that this bulk-derived LPS (BLPS) is capable of reproducing quite well NLPS predictions in KS-DFT calculations for bulk Si;¹² this new LPS type may prove to be of general utility in OF-DFT. If so, then we are left with the more intractable problem of constructing transferable KEDFs to evaluate the kinetic energy.

The KS-DFT “wave function” is a single determinant of one-electron orbitals, which are solutions of the following one-particle Schrödinger-like equations:

$$\left(-\frac{\nabla^2}{2} + v_{\text{eff}}(\mathbf{r}) \right) \phi_i(\mathbf{r}) = \epsilon_i \phi_i(\mathbf{r}), \quad (3)$$

where $v_{\text{eff}}(\mathbf{r})$ is the KS effective potential (containing the Hartree, exchange-correlation, and ion-electron potentials). The ground state in KS theory possesses the first-order reduced density matrix (DM1)^{7,13}

$$\gamma_1(\mathbf{r}, \mathbf{r}') = \sum_i \phi_i(\mathbf{r}) \phi_i^*(\mathbf{r}'), \quad (4)$$

which satisfies the following idempotency property:

$$\int \gamma_1(\mathbf{r}, \mathbf{r}'') \gamma_1(\mathbf{r}'', \mathbf{r}') d\mathbf{r}'' = \gamma_1(\mathbf{r}, \mathbf{r}'). \quad (5)$$

In KS theory,¹⁴ the kinetic energy in Eq. (1) can be calculated as

$$T_s^{\text{KS}}[\gamma_1(\mathbf{r}, \mathbf{r}')] = \frac{1}{2} \langle \nabla_{\mathbf{r}} \cdot \nabla_{\mathbf{r}'} \gamma_1(\mathbf{r}, \mathbf{r}') |_{\mathbf{r}=\mathbf{r}'} \rangle, \quad (6)$$

and the total energy can then be minimized with respect to KS orbitals $\phi_i(\mathbf{r})$. In OF-DFT, the KS orbitals are bypassed and the variational variable is reduced to the electron density ρ , at the cost of approximating the kinetic energy as well as the loss of the constraint in Eq. (5) on its underlying DM1. Consequently, there is no guarantee that a minimum of the total energy always exists in an OF-DFT formulation.^{13,15,16}

First-order perturbation theory tells us that an important constraint on KEDFs should be that they possess the correct linear-response (LR) behavior.¹⁷ Namely, a small change in the potential $\delta v(\mathbf{r})$ should produce a corresponding first-order change in the density $\delta \rho(\mathbf{r})$, given by

$$\delta \rho(\mathbf{r}) = \int \chi(\mathbf{r}-\mathbf{r}') \delta v(\mathbf{r}') d\mathbf{r}', \quad (7)$$

where $\chi(\mathbf{r}-\mathbf{r}')$ is the electron susceptibility function. Thus, if the perturbation is added to the total potential $v_{\text{eff}}(\mathbf{r})$ in Eq. (3), we have in reciprocal space

$$\begin{aligned} \hat{F} \left(\frac{\delta v_{\text{eff}}(\mathbf{r})}{\delta \rho(\mathbf{r}')} \right) &= \hat{F} \left(\frac{\delta^2 (E_v[\rho] - T_s[\rho])}{\delta \rho(\mathbf{r}') \delta \rho(\mathbf{r})} \right) \\ &= -\hat{F} \left(\frac{\delta^2 T_s[\rho]}{\delta \rho(\mathbf{r}') \delta \rho(\mathbf{r})} \right) = \frac{1}{\tilde{\chi}(\mathbf{q})}, \end{aligned} \quad (8)$$

where \hat{F} denotes the Fourier transform and $\tilde{\chi}(\mathbf{q})$ is the LR function in reciprocal space. Strictly speaking, $\tilde{\chi}(\mathbf{q})$ is system dependent. For a uniform electron gas of density ρ_0 , the analytic LR function was derived by Lindhard¹⁸ as

$$\begin{aligned} \tilde{\chi}_{\text{Lind}}(\mathbf{q}) &= -\frac{k_F}{\pi^2} \left(\frac{1}{2} + \frac{1-\eta^2}{4\eta} \ln \left| \frac{1+\eta}{1-\eta} \right| \right) \\ &= -\frac{k_F}{\pi^2} F_{\text{Lind}}^{-1}(\eta), \end{aligned} \quad (9)$$

where $k_F = (3\pi^2\rho_0)^{1/3}$ is the Fermi wave vector (FWV), $\eta = q/2k_F$ is a dimensionless momentum, and F_{Lind} is the Lindhard function. For nearly-free-electron systems with average density ρ_0 , inserting $\tilde{\chi}_{\text{Lind}}$ into Eq. (8) yields a relationship between the unspecified KEDF and the Lindhard response function

$$\hat{F} \left(\frac{\delta^2 T_s[\rho]}{\delta \rho(\mathbf{r}) \delta \rho(\mathbf{r}')} \Big|_{\rho_0} \right) = -\frac{1}{\tilde{\chi}_{\text{Lind}}} = \frac{\pi^2}{k_F} F_{\text{Lind}}(\eta), \quad (10)$$

which can be used to derive KEDFs that will satisfy LR theory for a perturbed uniform electron gas.

The design of KEDFs has a long history, with many KEDFs proposed for OF-DFT.^{7,19} Popular KEDFs include the TF^{8,20} KEDF, the von Weizsäcker²¹ (vW) KEDF and its extensions,²² and those based on the conventional gradient expansion^{16,23,24} (CGE) and generalized gradient approximation (GGA).²⁵ Not surprisingly, these KEDFs generate unsatisfactory results, since none of them have DM1s that obey the idempotency property of Eq. (5), nor do any of them have the correct LR behavior of Eq. (10). Since the late 1970s, more accurate KEDFs based on the weighted density approximation (WDA) and the average density approximation (ADA) have been proposed.^{26,27} In the WDA, the idempotency property is directly enforced for its DM1; in the ADA, the KEDF is constrained to have the correct LR. Encouraging results were achieved when such KEDFs were applied to atoms and spherical jellium surfaces.^{26,27} Unfortunately, an effective scheme utilizing these KEDFs more generally in OF-DFT is still lacking due to their complex structure. Reference 7 offers a detailed analysis of the above KEDFs with regard to the underlying DM1s and LR behavior for each category.

II. LINEAR-RESPONSE-BASED KINETIC ENERGY DENSITY FUNCTIONALS

First-principles methods that scale linearly with size are essential for large scale condensed matter calculations. In the last decade, several linear scaling LR-based KEDFs have been developed and shown to be quite successful for simple (nontransition) metals, which are nearly-free-electron-like.^{2,28–31}

A. LR-based KEDFs with a density-independent kernel

The LR-based KEDFs usually contain the TF and vW terms, as well as a third term meant to patch up the incorrect LR properties of the first two terms

$$T_s^{\alpha,\beta}[\rho] = T_{\text{TF}}[\rho] + T_{\text{vW}}[\rho] + T_X^{\alpha,\beta}[\rho]. \quad (11)$$

Both the TF and vW KEDFs can be recast in a general double-integral form

$$T_{\text{TF}}[\rho] = C_{\text{TF}} \langle \rho^{5/6}(\mathbf{r}) | \delta(\mathbf{r} - \mathbf{r}') | \rho^{5/6}(\mathbf{r}') \rangle, \quad (12)$$

$$T_{\text{vW}}[\rho] = -\frac{1}{4} \langle \rho^{1/2}(\mathbf{r}) | \delta(\mathbf{r} - \mathbf{r}') \nabla^2 + \nabla^2 \delta(\mathbf{r} - \mathbf{r}') | \rho^{1/2}(\mathbf{r}') \rangle, \quad (13)$$

with $C_{\text{TF}} = \frac{3}{10}(3\pi^2)^{2/3}$ in Eq. (12). It is natural then to propose a similar form for the third term^{7,31} in Eq. (11)

$$T_X^{\alpha,\beta}[\rho] = C_{\text{TF}} \langle \rho^\alpha(\mathbf{r}) | w(\rho_0, |\mathbf{r} - \mathbf{r}'|) | \rho^\beta(\mathbf{r}') \rangle. \quad (14)$$

This form allows the KEDF to be evaluated with fast Fourier transforms (FFTs),³² thereby leading to $O(N \ln N)$ scaling in the OF-DFT algorithm.

A basic ansatz for the DM1 (for more details, see Ref. 7) within LR theory is

$$\gamma_1^{\text{LR}}(\mathbf{r}, \mathbf{r}') = 3\rho^{1/2}(\mathbf{r})\rho^{1/2}(\mathbf{r}') \frac{j_1(\bar{y})}{\bar{y}}, \quad (15)$$

$$\bar{y}(\mathbf{r}, \mathbf{r}') = \bar{\xi}_{\text{F}}(\mathbf{r}, \mathbf{r}') |\mathbf{r} - \mathbf{r}'|, \quad (16)$$

$$\bar{\xi}_{\text{F}}(\mathbf{r}, \mathbf{r}') = \bar{\xi}_{\text{F}}[\bar{k}_{\text{F}}(\mathbf{r}), \bar{k}_{\text{F}}(\mathbf{r}')], \quad (17)$$

$$\bar{k}_{\text{F}}(\mathbf{r}) = (3\pi^2)^{1/3} \sqrt{\overline{\zeta^2(\mathbf{r})}}, \quad (18)$$

$$\overline{\zeta^2(\mathbf{r})} = \rho^{2/3}(\mathbf{r}) + \rho^{\alpha-1}(\mathbf{r}) \int w(\rho_0, |\mathbf{r} - \mathbf{r}'|) \rho^\beta(\mathbf{r}') d\mathbf{r}', \quad (19)$$

where j_1 is the spherical Bessel function and \bar{y} is the two-body natural variable.³³ $\bar{\xi}_{\text{F}}(\mathbf{r}, \mathbf{r}')$ is the average two-body Fermi wave vector (TBFVW), which depends on the average local FWV, \bar{k}_{F} , and it should satisfy

$$\lim_{\mathbf{r}' \rightarrow \mathbf{r}} \bar{\xi}_{\text{F}}(\mathbf{r}, \mathbf{r}') = \bar{k}_{\text{F}}(\mathbf{r}). \quad (20)$$

$\overline{\zeta^2(\mathbf{r})}$ is the average FWV squared and the averaging weight function (AWF), $w(\rho_0, |\mathbf{r} - \mathbf{r}'|)$, allows nonlocal effects to be built into the LR KEDF.⁷ If one inserts this DM1 of Eqs. (15)–(19) into Eq. (6), one recovers Eq. (11), the definition of the LR-based KEDF. Therefore this DM1 is of the correct

form to recover LR behavior, though this form of DM1 may not be the only (unique) form for LR-based KEDFs.⁷

In order for all the quantities in Eqs. (15)–(19) to have reasonable values, at least $\overline{\zeta^2(\mathbf{r})}$ must be semipositive definite everywhere. This requirement may be satisfied for nearly-free-electron systems, however, as we shall see, $\overline{\zeta^2(\mathbf{r})}$ may become negative during iterative solution of the TFHK equation [Eq. (2)] for systems involving large density fluctuations. If so, the variational search may enter an unphysical space.

Several sets of values have been proposed for the two parameters α and β that appear in the above KEDF.^{2,28–30} The Wang-Teter (WT) KEDF²⁸ selects $\alpha = \beta = \frac{5}{6}$, the Perrot KEDF²⁹ has $\alpha = \beta = 1$, the Smargiassi-Madden KEDF² chooses $\alpha = \beta = \frac{1}{2}$, and the Wang-Govind-Carter (WGC) KEDF (Ref. 30) with a density-independent kernel offers other choices of α and β . A detailed analysis of these KEDFs can be found in Ref. 30.

B. WGC KEDF with a density-dependent kernel

Wang *et al.* made further improvements upon the above LR KEDFs by introducing a density dependence into the kernel w through the nonlocal TBFVW $\xi_\gamma(\mathbf{r}, \mathbf{r}')$, which depends on the local one-body FWV $k_{\text{F}}(\mathbf{r})$ and involves a mixing parameter γ .^{7,31}

$$\xi_\gamma(\mathbf{r}, \mathbf{r}') = \left(\frac{k_{\text{F}}^\gamma(\mathbf{r}) + k_{\text{F}}^\gamma(\mathbf{r}')}{2} \right)^{1/\gamma}, \quad (21)$$

where $k_{\text{F}}(\mathbf{r}) = [3\pi^2\rho(\mathbf{r})]^{1/3}$. Replacing ρ_0 in the AWF w of Eq. (14) by $\xi_\gamma(\mathbf{r}, \mathbf{r}')$, one obtains the WGC KEDF

$$T_s^{\alpha,\beta,\gamma} = T_{\text{TF}}[\rho] + T_{\text{vW}}[\rho] + T_{\text{WGC}}^{\alpha,\beta,\gamma}[\rho], \quad (22)$$

where

$$T_{\text{WGC}}^{\alpha,\beta,\gamma}[\rho] = C_{\text{TF}} \langle \rho^\alpha(\mathbf{r}) | w_{\alpha,\beta}[\xi_\gamma(\mathbf{r}, \mathbf{r}'), |\mathbf{r} - \mathbf{r}'|] | \rho^\beta(\mathbf{r}') \rangle. \quad (23)$$

The introduction of the symmetric TBFVW $\xi_\gamma(\mathbf{r}, \mathbf{r}')$ into the kernel of Eq. (23) renders the new version of the WGC KEDF more transferable than the previous one³⁰ with a density-independent kernel. However, the complex structure of the new WGC KEDF is a disadvantage in practice. In order to define the corresponding DM1, one only needs to replace Eq. (19) by the following:

$$\overline{\zeta^2(\mathbf{r})} = \rho^{2/3}(\mathbf{r}) + \rho^{\alpha-1}(\mathbf{r}) \int w[\xi_\gamma(\mathbf{r}, \mathbf{r}'), |\mathbf{r} - \mathbf{r}'|] \times \rho^\beta(\mathbf{r}') d\mathbf{r}'. \quad (24)$$

Equations (23) and (24) should be less approximate than Eqs. (14) and (19), since the electron densities at \mathbf{r} and \mathbf{r}' are not likely to be ρ_0 for systems involving large density fluctuations. Moreover, the AWF w should depend on the nonlocal TBFVW $\xi(\mathbf{r}, \mathbf{r}')$, which is a function of $k_{\text{F}}(\mathbf{r})$ and $k_{\text{F}}(\mathbf{r}')$ instead of simply $k_{\text{F}}(\rho_0)$. Finally, the particular choice of the form for the TBFVW $\xi_\gamma(\mathbf{r}, \mathbf{r}')$ in Eq. (21) has been justified by the analysis of natural variables for density functionals,^{7,33} although it is not a unique choice.

The kernel in Eqs. (23) and (24) can be evaluated in reciprocal space via the Fourier transform

$$w[\xi_\gamma(\mathbf{r}, \mathbf{r}'), |\mathbf{r} - \mathbf{r}'|] = \frac{1}{\Omega} \sum_{\mathbf{g}} w(\eta) e^{-i\mathbf{g} \cdot (\mathbf{r} - \mathbf{r}')}, \quad (25)$$

where Ω is the volume of the simulation cell and η is the reciprocal space wave vector \mathbf{g} scaled by the TBFVW $\xi_\gamma(\mathbf{r}, \mathbf{r}')$

$$\eta = \frac{\mathbf{g}}{2\xi_\gamma(\mathbf{r}, \mathbf{r}')} \quad (26)$$

Enforcing LR theory for a uniform electron gas of density ρ_0 naturally leads to the inhomogeneous Cauchy-Euler equation for the WGC kernel in reciprocal space³¹

$$\eta^2 \bar{w}''_{\alpha,\beta}(\eta, \rho_0) + (1-2p)\eta \bar{w}'_{\alpha,\beta}(\eta, \rho_0) + (p^2-q)\bar{w}_{\alpha,\beta}(\eta, \rho_0) = 20G(\eta)\rho_0^{5/3-(\alpha+\beta)}, \quad (27)$$

$$p = 3(\alpha + \beta) - \gamma/2, \quad (28)$$

$$q = p^2 - 36\alpha\beta, \quad (29)$$

$$G(\eta) = F_{\text{Lind}}(\eta) - 3\eta^2 - 1. \quad (30)$$

Note that if $\alpha + \beta = \frac{5}{3}$, the dependence of Eq. (27) on ρ_0 is removed. The solution of Eq. (27) includes a general analytic part and a specific power series part, which allows the reciprocal space AWF \bar{w} to be evaluated to arbitrary accuracy.⁷

By Fourier transforming the reciprocal space kernel \bar{w} into real space and then substituting the result into Eqs. (22) and (23), one obtains the asymptotic behavior of $T_s^{\alpha,\beta,\gamma}$ for the $q \rightarrow 0$ limit³¹

$$\begin{aligned} T_s^{\alpha,\beta,\gamma} \rightarrow T_{\text{TF}} + (1 + \lambda_0)T_{\text{vW}} + \lambda_0(\alpha + \beta - 1)\langle \delta\sigma | t_{\text{vW}} \rangle \\ + \frac{\lambda_0}{2}(\alpha + \beta - 1)(\alpha + \beta - 2)\langle \delta\sigma^2 | t_{\text{vW}} \rangle \\ + o(\delta\sigma^3), \end{aligned} \quad (31)$$

where

$$\lambda_0 = \frac{-8\alpha\beta}{9\alpha\beta - p + 1}, \quad (32)$$

and for the $q \rightarrow \infty$ limit³¹

$$\begin{aligned} T_s^{\alpha,\beta,\gamma} \rightarrow T_{\text{vW}} + (1 + \lambda_\infty)T_{\text{TF}} + \lambda_\infty \left(\alpha + \beta - \frac{5}{3} \right) \langle \delta\sigma | t_{\text{TF}} \rangle \\ + \frac{\lambda_\infty}{2} \left(\alpha + \beta - \frac{5}{3} \right) \left(\alpha + \beta - \frac{8}{3} \right) \langle \delta\sigma^2 | t_{\text{TF}} \rangle \\ + o(\delta\sigma^3), \end{aligned} \quad (33)$$

where

$$\lambda_\infty = \frac{-8}{9\alpha\beta}. \quad (34)$$

We note that the corresponding equations in Ref. 7 [Eqs. (168)–(171)] and Ref. 31 [Eqs. (27)–(30)] are only correct for $\alpha + \beta = \frac{5}{3}$. Our results here are general for any possible choice of α and β . Using the $(5/6) \pm (\sqrt{5}/6)$ for α and β proposed by Wang *et al.*,³¹ $T_s^{\alpha,\beta,\gamma}$ reproduces the correct large q limit:^{7,30} $T_{\text{vW}} - \frac{2}{3}T_{\text{TF}}$ for $q \rightarrow \infty$, where the spurious terms involving various orders of $\delta\sigma$ in Eq. (33) vanish.³¹ For the $q \rightarrow 0$ limit [Eq. (31)], choosing $\gamma = 8$ allows $T_s^{\alpha,\beta,\gamma}$ to reproduce the second-order CGE,²³ however, in this case the spurious terms cannot be well controlled. Thus, the opti-

mal value for γ is unfortunately system dependent. For Al crystals, surfaces, and defects, Wang *et al.* varied the value of γ and found that $\gamma = 2.7$ yielded optimal results.³¹

For $\{\alpha, \beta = (5/6) \pm (\sqrt{5}/6)\}$, the solution of Eq. (27) depends on the value of γ , falling into one of the following six categories characterized by the sign of p and q : (a) $p > 0, q > 0$ when $0 < \gamma < 1.0557$; (b) $p > 0, q = 0$ when $\gamma = 1.0557$; (c) $p > 0, q < 0$ when $1.0557 < \gamma < 10.0$; (d) $p < 0, q < 0$ when $10.0 < \gamma < 18.9443$; (e) $p < 0, q = 0$ when $\gamma = 18.9443$; and (f) $p < 0, q > 0$ when $\gamma > 18.9443$. If $\gamma = 10$, the general solution of Eq. (27) diverges as $\eta \rightarrow 0$ and as $\eta \rightarrow \infty$. In this work, the value of γ chosen is in category (c), as shown in Table I in Sec. III D. We also tried γ in other value ranges, however the results were not promising, at least for bulk silicon. Lastly, we note that changes in γ affect the shape of $\eta^2 \bar{w}''$ more than the shape of \bar{w} or $\eta \bar{w}'$ in reciprocal space.

C. Taylor expansion of the WGC response kernel

Unfortunately, the density dependence in the kernel makes the direct evaluation of the WGC kinetic energy with FFTs impossible. To achieve linear scaling, the following Taylor series expansion was proposed by Wang *et al.*³¹ to factor out the density dependence in the kernel:

$$\begin{aligned} w_{\alpha,\beta}[\xi_\gamma(\mathbf{r}, \mathbf{r}'), |\mathbf{r} - \mathbf{r}'|] \\ = w_{\alpha,\beta}[k_{\text{F}}^*, |\mathbf{r} - \mathbf{r}'|] + \left. \frac{\partial w_{\alpha,\beta}[\xi_\gamma(\mathbf{r}, \mathbf{r}'), |\mathbf{r} - \mathbf{r}'|]}{\partial \rho(\mathbf{r})} \right|_{\rho_*} \theta(\mathbf{r}) \\ + \left. \frac{\partial w_{\alpha,\beta}[\xi_\gamma(\mathbf{r}, \mathbf{r}'), |\mathbf{r} - \mathbf{r}'|]}{\partial \rho(\mathbf{r}')} \right|_{\rho_*} \theta(\mathbf{r}') \\ + \left. \frac{\partial^2 w_{\alpha,\beta}[\xi_\gamma(\mathbf{r}, \mathbf{r}'), |\mathbf{r} - \mathbf{r}'|]}{\partial \rho^2(\mathbf{r})} \right|_{\rho_*} \frac{\theta^2(\mathbf{r})}{2} \\ + \left. \frac{\partial^2 w_{\alpha,\beta}[\xi_\gamma(\mathbf{r}, \mathbf{r}'), |\mathbf{r} - \mathbf{r}'|]}{\partial \rho^2(\mathbf{r}')} \right|_{\rho_*} \frac{\theta^2(\mathbf{r}')}{2} \\ + \left. \frac{\partial^2 w_{\alpha,\beta}[\xi_\gamma(\mathbf{r}, \mathbf{r}'), |\mathbf{r} - \mathbf{r}'|]}{\partial \rho(\mathbf{r}) \partial \rho(\mathbf{r}')} \right|_{\rho_*} \theta(\mathbf{r}) \theta(\mathbf{r}') + \dots, \end{aligned} \quad (35)$$

where $\theta(\mathbf{r}) = \rho(\mathbf{r}) - \rho_*$, and ρ_* is a reference density, usually chosen to be the average density ρ_0 of the system. Note that the Taylor expansion can only be carried out to second order, since the third derivative of \bar{w} involves the first derivative of the Lindhard function, which has a logarithmic discontinuity at $\eta = 1$. The coefficients of the first- and second-order terms can be evaluated in reciprocal space via FFT [see Eqs. (43)–(45) in Ref. 31], and the WGC KEDF can be evaluated in reciprocal space via a series of six FFTs. In regions of large density fluctuations, the above truncated Taylor expansion, Eq. (35), may not be converged at second order. This in turn can lead to convergence problems during iterative solution of the TFHK equation, as will be shown in Sec. III B.

When the WGC KEDF is used in OF-DFT calculations, we have shown that we can quantitatively reproduce KS-DFT results for near-free-electron-like simple metals and alloys.^{31,34} For Al surfaces and vacancies, which are not par-

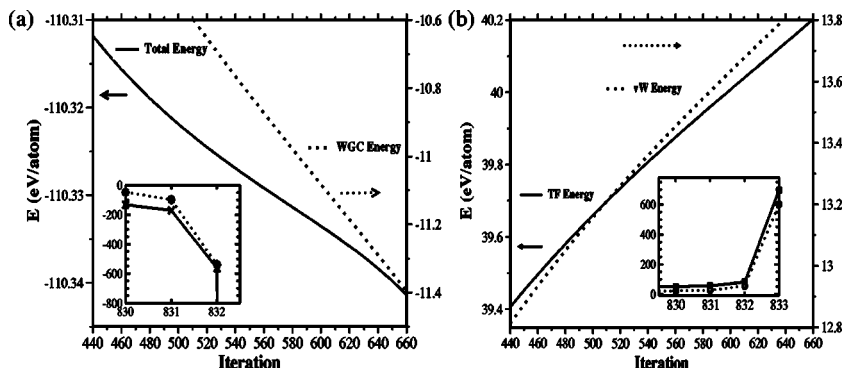


FIG. 1. Data from an OF-DFT calculation using the WGC KEDF ($\gamma=2.7$, from Ref. 12) on CD Si with a lattice constant of 5.385 Å. (a) The total energy (solid) and WGC portion (dotted) of the kinetic energy at each iteration. Inset: the total energy and WGC portion of the kinetic energy at the last three iteration steps (symbols). (b) The TF (solid) and vW portion (dotted) of the kinetic energy at each iteration. Inset: the TF and vW portion of the kinetic energy at the last four iteration steps (symbols). In both insets, the two sets of data are on the same scale.

ticularly free-electron-like, the WGC KEDF produces results that are much more accurate than other LR-based KEDFs.³¹ It is, for better or worse, the state-of-the-art linear scaling KEDF today. Our challenge here is to determine if the WGC KEDF, combined with the recently developed BLPS,¹² can produce reasonable properties of covalent materials when used within OF-DFT calculations.

III. OF-DFT CALCULATIONS FOR CRYSTALLINE Si

Here we employ the WGC KEDF combined with a BLPS in OF-DFT calculations on various crystalline phases of bulk Si. Earlier,¹² we reported that the OF-DFT calculations do not converge well for cubic diamond (CD), hexagonal diamond (HD), and complex body-center cubic (cbcc) structures. We used a second-order damped dynamics method,^{7,31} which had a very small convergence radius, resulting in a high computational cost due to the large number of iterations required. In addition to the convergence issue, the OF-DFT predictions deviated significantly from conventional KS-DFT results, especially for the semiconducting phases (CD and HD).¹² The convergence problem may be due in part to the truncation of the Taylor series expansion for the WGC response kernel \tilde{w} . However, we will see that a defect in the DM1 ansatz underlying the LR KEDFs is responsible for the quantitative errors. We further show that it is possible to optimize the values of γ and ρ_* so as to semi-quantitatively reproduce KS-DFT equations of state (EOS) for various bulk phases of Si within OF-DFT. This was not possible before, when we employed the value of γ optimal for nearly-free-electron-like metals ($\gamma=2.7$). We also used the WT KEDF²⁸ in OF-DFT for comparison purposes.

A. Computational details

We use the local density approximation (LDA) to electron exchange and correlation, which is based on the quantum Monte Carlo results of Ceperley and Alder, as parametrized by Perdew and Zunger.³⁵ For bulk properties of crystals, it has been shown that the LDA is sufficient and that improvement in predictive capability is not guaranteed by utilizing the GGA.³⁶ The CASTEP code³⁷ was used to run KS-LDA calculations, using either Troullier-Martins NLPSs¹¹ or the recently developed BLPSs¹² to calculate the external potential energy. A kinetic energy cutoff of 760 eV was employed in KS-DFT calculations, resulting in convergence of the total energy to ~ 0.004 – 0.014 eV/atom,

depending on the phase examined. In OF-DFT calculations, the BLPS was used to calculate the external potential energy. A kinetic energy cutoff of 1520 eV was employed to converge the representation of the OF-DFT electron density.

We studied nine different bulk phases of Si crystals: CD, HD, cbcc, β tin, body-centered tetragonal (bct5), simple cubic (sc), simple bcc (sbcc), face-centered cubic (fcc), and hexagonal-close-packed (hcp).^{38,39} The simulation cells for each of these phases contained 2, 4, 8, 2, 4, 1, 1, 1, and 2 atoms in KS-DFT calculations (primitive cells) and 8, 8, 16, 4, 4, 8, 2, 4, and 4 atoms in OF-DFT calculations (cubic cells), respectively. Detailed descriptions of the structures are given in Ref. 12. The Monkhorst-Pack method was employed to generate special \mathbf{k} points for the Brillouin-zone sampling⁴⁰ required in KS calculations on periodic systems. The number of \mathbf{k} points used in the irreducible Brillouin zones are 28, 36, 60, 120, 112, 84, 120, 84, and 64 for primitive cells of the CD, HD, cbcc, β tin, bct5, sc, sbcc, fcc, and hcp phases, respectively.

A second-order damped dynamics method^{7,31} was employed to minimize the total energy in the OF-DFT calculations. Several different convergence criteria were used (see Ref. 12 and Table I in Sec. III D). As we shall see, the numerical instability of the Taylor series expansion for the WGC kernel forces us to use a loose convergence criterion for CD, HD, and cbcc bulk phases. When the WT KEDF is used, the OF-DFT total energy convergence criterion can be set to 0.001 meV/atom for all bulk structures.

B. The convergence problem due to the Taylor series expansion

Tests were performed within OF-DFT on CD Si using the KS-LDA/NLPS equilibrium lattice constant of 5.385 Å. The total energy diverges during minimization, as illustrated by the solid curve in Fig. 1(a). Similar behavior is also observed for the WGC portion of the kinetic energy, $T_{\text{WGC}}^{\alpha,\beta,\gamma}[\rho]$, from Eq. (23) (dotted curve). The inset demonstrates that at the last three iteration steps, the total energy diverges catastrophically and the WGC portion of the kinetic energy dominates all other energy components at the last step. Figure 1(b) displays the divergence of TF and vW kinetic energies at intermediate and late stages of the self-consistent loop. We see that once the WGC term diverges towards $-\infty$, the TF and vW terms diverge towards $+\infty$ at the same time.

Interestingly, if the Taylor series expansion of the WGC

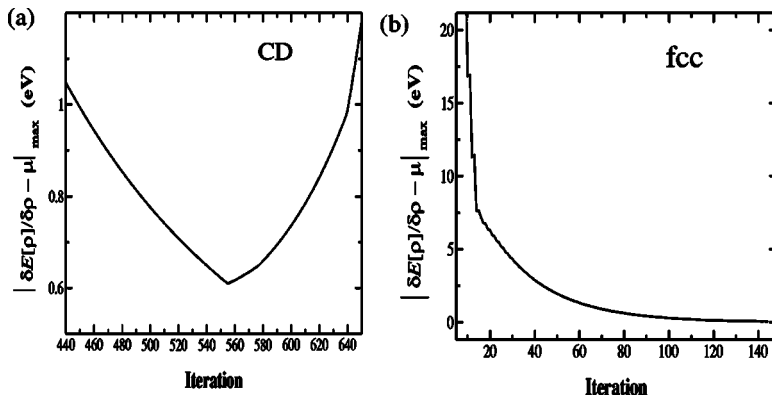


FIG. 2. The maximum absolute deviation of the total potential $\delta E[\rho]/\delta\rho$ from the chemical potential μ during OF-DFT iterations using the WGC KEDF with $\gamma = 2.7$ from Ref. 7. (a) CD Si; (b) fcc Si.

response kernel \tilde{w} [Eq. (35)] is only carried out to first order, the OF-DFT calculation fully converges. This indicates that the numerical divergence is mainly caused by the second-order contribution of the truncated Taylor series expansion. Though the third-order contribution might counteract the second-order contribution, as mentioned before we cannot go to higher orders in the Taylor expansion due to the logarithmic discontinuity in the first-order derivative of the Lindhard function.

To further track down the convergence problem, we examined the behavior of the difference between the total potential and the Lagrange multiplier (which becomes the chemical potential after the total energy is minimized), $\{\delta E[\rho]/\delta\rho(\mathbf{r})\} - \mu$, which should converge to zero [Eq. (2)]. We evaluate this latter quantity on the whole grid and take the value at the grid point that is the maximum in absolute value at each iteration. Figure 2(a) illustrates that for CD Si up iteration step 550, $\{\delta E[\rho]/\delta\rho\} - \mu|_{\max}$ decreased as expected. However, it then starts to increase instead of decreasing towards zero. This abnormal behavior of the total potential is very likely caused by the truncated Taylor expansion of the WGC potential at second order. By contrast, $\{\delta E[\rho]/\delta\rho(\mathbf{r})\} - \mu|_{\max}$ for fcc Si decreased until it vanished [Fig. 2(b)], suggesting no divergence in the WGC potential for metallic phases.

We also investigated the real space distribution of $\{\delta E[\rho]/\delta\rho\} - \mu$ at two representative iteration steps (Fig. 3), along the diagonal direction of (110) plane of CD Si. At iteration step 500 (solid line; before divergence), $\{\delta E[\rho]/\delta\rho\} - \mu$ in the interstitial area [$2.4 \text{ \AA} \leq r \leq 9.4 \text{ \AA}$] is larger than in the Si-Si bond region [$0.4 \text{ \AA} \leq r \leq 2.0 \text{ \AA}$]. One hundred and fifty steps later (after divergence), $\{\delta E[\rho]/\delta\rho\} - \mu$ in the interstitial area has decreased, while in the Si-Si bond region it has diverged (dashed line). This indicates that it is in the Si-Si bond regions, where $\rho(\mathbf{r})$ is much larger than ρ_* , that the abnormal divergence behavior of the total potential $\{\delta E[\rho]/\delta\rho\}$ is very likely to occur. This also explains the well-behaved convergence behavior of metallic fcc Si, where $\rho(\mathbf{r})$ never deviates strongly from ρ_* , and hence the Taylor expansion there is well justified.

As noted before, the shape of the reciprocal space kernel \tilde{w} , especially its second-order derivative \tilde{w}'' , is sensitive to the choice of γ . The parameter γ certainly influences the convergence properties of the KEDF. Indeed, we find that OF-DFT calculations using the WGC KEDF for CD Si can

be much better converged when $4.0 \leq \gamma < 10.0$ rather than $\gamma = 2.7$, as discussed below. We also find that the convergence properties are affected by the choice of reference density ρ_* .

C. The behavior of the average FWV squared

As mentioned in Sec. II A, in order for the DM1 underlying the LR KEDFs to be physically meaningful, at least the average FWV squared $\bar{\zeta}^2$ should be semipositive definite everywhere in space. It turns out that this is not guaranteed, even with the enforcement of the correct LR. Figure 4 displays the minimum of the average FWV squared, $\bar{\zeta}_{\min}^2$ [Eq. (24)], for CD and fcc Si as the iterations proceed. The solid lines are from $\{\gamma = 2.7, \rho_* = \rho_0\}$ and the dashed lines are from the optimal parameter set (see the following section). We see in Fig. 4(a) that after iteration step 150, $\bar{\zeta}_{\min}^2$ from both parameter sets become negative for CD Si. Consequently, the variational search enters an unphysical space, in which there is no guarantee that a minimum of the total energy exists. This explains the divergence of the total energy to a very negative number in Fig. 1(a). However, $\bar{\zeta}_{\min}^2$ from the optimal parameter set drifts to negative values in a slower fashion. By contrast, $\bar{\zeta}_{\min}^2$ always stays positive for fcc Si during OF-DFT iterations, because metallic phases of Si are still in the LR regime and therefore well behaved. In this case, little difference between $\bar{\zeta}_{\min}^2$ from the two parameter sets can be seen.

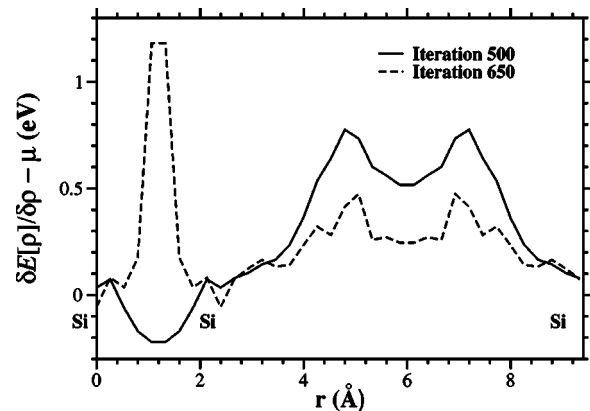


FIG. 3. Deviation of the total potential $\delta E[\rho]/\delta\rho$ from chemical potential μ along the diagonal of (110) plane of CD Si in OF-DFT using the WGC KEDF with $\gamma = 2.7$. Iteration step 500 (solid) and 650 (dashed) are shown.

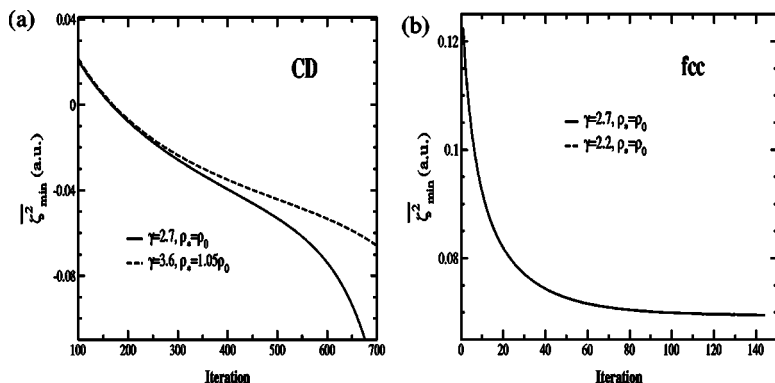


FIG. 4. The minimum of the average Fermi wave vector squared $\bar{\zeta}_{\min}^2$ during OF-DFT iterations using the WGC KEDF with $\{\gamma=2.7, \rho_*=\rho_0\}$ (solid line) and optimal parameter set (dashed line). (a) CD Si; (b) fcc Si.

D. Searching for the optimal γ and reference density ρ_*

Despite the divergence problem, we explored parameter space to search for optimal values of γ and ρ_* , using as figures of merit the KS/BLPS EOSs of different bulk phases of Si. Table I lists the optimal values found for γ and ρ_* for various bulk phases of Si, as well as the best convergence we can achieve in each case within OF-DFT with a Si BLPS. We find the optimal choice of γ depends on whether the system under study is a semiconductor or a metal, while the optimal choice of ρ_* depends on the coordination number. The original parameters suggested for aluminum $\{\gamma=2.7, \rho_*=\rho_0\}$ are not the best choice for any structures of Si. As reported in Ref. 12, the largest errors from OF-DFT calculations lie in the EOSs of semiconducting phases, CD, and HD. Significant improvements to the EOSs are made using 3.6 instead of 2.7 for γ , as will be shown in the following section. The use of $\gamma=2.2$ is optimal for the metallic phases. The reference density ρ_* is usually chosen to be the average density ρ_0 . Interestingly, better EOSs are obtained for structures of low coordination number (≤ 6) from using $\rho_*=1.05\rho_0$, though the resulting variational density sometimes degrades slightly. Although the use of optimal parameter set cannot prevent the average FWV $\bar{\zeta}^2$ from becoming negative for semiconducting phases, it does slow down this negative behavior [see Fig. 4(a)]. Unfortunately, no universal values exist for γ and ρ_* that are best for all structures. We suggest the use of the optimal parameters found here as recommended compromise parameters for future practical applications, based on the results presented in the following section.

The OF-DFT calculations can be fully converged for all bulk structures but three: CD, HD, and cbc. It is striking that these are the three structures with the lowest coordination number (see Table I). The density distributions in these structures are the least spherically symmetric and most local-

ized. This puts a heavy burden on the ability of the truncated Taylor series expansion for the WGC KEDF potential to converge well. If alternatives to a Taylor series expansion could be found that retain linear scaling, these would be a superior approach to the evaluation of KEDFs for covalent materials. Such algorithms might allow the corresponding KEDF potential to converge well even for large density fluctuations.

IV. APPLICATION OF THE WGC KEDF TO Si USING OPTIMAL γ AND ρ_*

Here we report OF-DFT predictions of bulk properties for nine phases of Si using the BLPS and the WGC KEDF with optimal values of γ and ρ_* , i.e., $\gamma=3.6$ for semiconductors and $\gamma=2.2$ for metals; $\rho_*=1.05\rho_0$ for low coordination number phases (≤ 6); and $\rho_*=\rho_0$ for high coordination number phases (> 6). We compare these results to those obtained using our earlier $\{\gamma=2.7, \rho_*=\rho_0\}$ (Ref. 12) for the WGC KEDF, as well as to those obtained from the WT KEDF.²⁸ KS/BLPS EOSs are used as benchmarks.

EOSs for CD and fcc Si within OF-DFT are compared to those from KS-DFT in Fig. 5. It is evident from Fig. 5(a) that the shape of EOS of CD Si using the optimal parameters in OF-DFT is much better than that obtained using the earlier set optimized for Al $\{\gamma=2.7, \rho_*=\rho_0\}$. Both manifest the superiority of the WGC KEDF to the WT KEDF, since both EOSs have clear minima [see insets of Fig. 5(a)] unlike the WT EOS. However, the EOSs from the WGC KEDF still contain significant errors, even using the optimal parameters. Figure 5(b) shows that both the WGC KEDF, using the original set $\{\gamma=2.7, \rho_*=\rho_0\}$ and the optimal set $\{\gamma=2.2, \rho_*=\rho_0\}$, as well as the WT KEDF, generate much better EOSs for fcc Si in OF-DFT. This is to be expected, since both KEDFs should perform well for metallic phases. The fcc Si EOS resulting from the optimal parameter set is only slightly better than that from the original parameter set.

TABLE I. Optimal mixing parameter γ and reference density ρ_* for various bulk phases of Si. c.n., coordination number; c.c., convergence criterion.

	CD	HD	cbcc	β tin	bct5	sc	hcp	sbcc	fcc
c.n.	4	4	4	6	5	6	12	8	12
γ	3.6	3.6	2.2	2.2	2.2	2.2	2.2	2.2	2.2
ρ_*/ρ_0	1.05	1.05	1.05	1.05	1.05	1.05	1.0	1.0	1.0
c.c. (meV/atom)	0.0625	0.5	0.0625	0.001	0.001	0.001	0.001	0.001	0.001

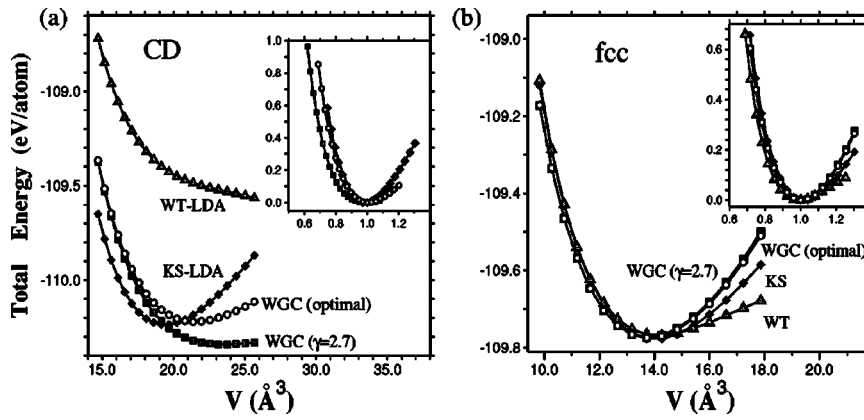


FIG. 5. LDA total energies (eV/atom) vs atomic volume (\AA^3) for CD (a) and fcc (b) Si. Insets: the total energy is shifted by the equilibrium atomic energy and the atomic volume is scaled by dividing by the equilibrium atomic volume. Here we compare KS/BLPS (solid diamonds) to OF/WGC KEDF (optimal γ and ρ_* ; open circles), to OF/WGC KEDF ($\gamma=2.7, \rho_* = \rho_0$; dark squares), to OF/WT KEDF (opaque triangles).

In order to obtain static structural properties, the EOS data were fitted to Murnaghan's equation of state⁴¹

$$E_{\text{tot}}(V) = \frac{B_0 V}{B'_0} \left(\frac{(V_0/V)^{B'_0}}{B'_0 - 1} + 1 \right) + \text{const}, \quad (36)$$

where B_0 and B'_0 are the bulk modulus and its pressure derivative at the equilibrium volume V_0 , respectively. Table II compares the static structural properties obtained from KS-LDA using both the NLPS and the BLPS to those from OF-LDA using the BLPS and the WGC KEDF with either the original $\{\gamma=2.7, \rho_* = \rho_0\}$ or the optimal parameters.

As reported earlier,¹² the BLPS results agree very well with those from the NLPS within KS-DFT. The relative error in equilibrium volume V_0 and bulk modulus B_0 are within 1% and 7%, respectively. The energy gap between the semiconducting and metallic phases of $\sim 0.15\text{--}0.45$ eV/atom predicted using the NLPS is well reproduced by the BLPS. The phase ordering from the BLPS is correct for almost all phases except that the energy of β -tin phase is ~ 0.05 eV/atom too high.

Use of the WGC KEDF with the original parameter set $\{\gamma=2.7, \rho_* = \rho_0\}$ in OF-DFT leads to significant errors in property prediction compared to KS NLPS results. The largest errors occur for CD Si, with errors in the equilibrium volume of $\sim 20\%$, in the bulk modulus of $\sim 70\%$, and in the equilibrium energy of ~ -0.1 eV/atom. The predicted OF equilibrium volumes and bulk moduli for the other phases are considerably more accurate, with errors $\leq 2\%$ for the former and $\leq 25\%$ for the latter. However, the energy differences between phases ΔE_{min} are too high and the phase ordering is wrong.

Significant improvements are seen in OF-DFT predictions for each phase using the optimal parameters in the WGC KEDF. The largest errors (relative to KS NLPS results) are still observed for CD Si, with errors in its equilibrium volume of $\sim 10\%$ and its bulk modulus of $\sim 35\%$. However, these errors are much smaller than those using $\{\gamma=2.7, \rho_* = \rho_0\}$. The errors in the equilibrium volume and bulk modulus for other phases are within 5% and 23%, respectively. The energy differences ΔE_{min} among the phases

TABLE II. KS (NLPS and BLPS) and OF (BLPS) LDA predictions of Si bulk properties: equilibrium volume V_0 , bulk modulus B_0 , equilibrium total energy for CD Si E_{min} , and equilibrium total energy relative to CD Si, $\Delta E_{\text{min}} = E_{\text{min}} - E_{\text{min}}^{\text{CD}}$, for other bulk phases. In OF-DFT, the WGC KEDF with $\{\gamma=2.7, \rho_* = \rho_0\}$ and optimal parameters (Table I) are used. The KS and OF results using the BLPS and the WGC KEDF ($\gamma=2.7, \rho_* = \rho_0$) were published in Ref. 12 and are reproduced here for ease of comparison.

	CD	HD	cbcc	β tin	bct5	sc	hcp	sbcc	fcc
KS NLPS									
V_0 (\AA^3)	19.532	19.579	17.735	14.796	16.871	15.499	13.765	14.057	13.850
B_0 (GPa)	92.5	89.2	90.8	114.7	98.2	105.0	89.0	96.6	86.7
$(\Delta)E_{\text{min}}$ (eV/atom)	-108.059	0.014	0.137	0.228	0.246	0.293	0.435	0.446	0.461
KS BLPS									
V_0 (\AA^3)	19.432	19.492	17.850	14.880	16.838	15.537	13.858	14.058	14.022
B_0 (GPa)	95.5	91.5	90.0	106.5	97.5	103.0	83.0	88.6	87.8
$(\Delta)E_{\text{min}}$ (eV/atom)	-110.234	0.020	0.165	0.275	0.249	0.303	0.447	0.462	0.457
OF BLPS, $\gamma=2.7$									
V_0 (\AA^3)	23.966	18.788	17.802	14.638	16.963	15.749	13.689	13.938	13.738
B_0 (GPa)	25.8	92.6	93.2	120.7	88.6	107.7	111.6	107.2	101.6
$(\Delta)E_{\text{min}}$ (eV/atom)	-110.345	0.324	0.537	0.515	0.602	0.506	0.569	0.617	0.571
OF BLPS, optimal γ, ρ_*									
V_0 (\AA^3)	21.585	19.676	18.372	15.098	17.695	16.156	13.713	13.965	13.763
B_0 (GPa)	60.9	76.7	87.9	104.4	77.8	95.5	109.6	105.4	99.8
$(\Delta)E_{\text{min}}$ (eV/atom)	-110.220	0.288	0.267	0.361	0.307	0.308	0.443	0.490	0.444

are now within ~ 0.1 eV/atom of the KS BLPS results except for HD phase, which is too high in energy. Overall, the energy gap of ~ 0.45 eV between the semiconducting and metallic phases is well reproduced with this new set of parameters for the WGC KEDF. Given the quite high accuracy of the BLPS with KS-DFT, these errors in the OF-DFT predictions should be attributed to remaining inherent deficiencies in the WGC KEDF.

V. SUMMARY AND CONCLUSIONS

The present state of OF-DFT in condensed matter is that it is reliable only for nearly-free-electron-like metals. The objective of the current work was to examine if an improved parametrization of a recently proposed KEDF, the WGC KEDF, may extend the reliability of OF-DFT to covalent materials.

The unique feature of the WGC KEDF is the introduction of a density dependence into its response kernel. In order to retain linear scaling of the OF-DFT algorithm when this WGC KEDF is employed, a Taylor series expansion is used to evaluate the WGC kernel at some reference density ρ_* , usually chosen to be the average density ρ_0 of the system. We demonstrated that this expansion can lead to numerical instabilities for systems with large fluctuations in the electron density (such as covalent materials with localized bonds). Further analysis reveals that the second-order contribution to the (necessarily truncated) Taylor expansion of the WGC KEDF response kernel is responsible for total energy divergence in such cases.

Neither the value of the mixing parameter γ in the WGC KEDF, nor the value of the reference density ρ_* in the Taylor expansion, are determined universally by asymptotic analysis (unlike the only other two parameters α and β of the WGC KEDF). Moreover, we find that the optimal values for γ and ρ_* depend, respectively, on whether the system is a semiconductor or a metal and on the coordination number. By optimizing the value of γ and ρ_* , semiquantitative results for bulk Si properties are obtained within OF-DFT. We recommend using these new parameters in the WGC KEDF whenever OF-DFT will be applied to nonmetallic systems. One serious problem with the WGC KEDF is the defect in its corresponding first-order reduced density matrix, in which a negative average FWV squared $\bar{\zeta}^2$ arises for localized densities. Unfortunately, use of an optimal parameter set did not entirely rectify this flaw. We attribute the major errors in OF-DFT to limitations of the WGC KEDFs. How to further improve the LR-based KEDFs so that systems with localized electron distributions can be described accurately remains at the frontier of the OF-DFT field.

ACKNOWLEDGMENTS

The authors thank Professor Yan Alexander Wang (University of British Columbia) for private communications and help with one of their OF-DFT codes. Financial support for this project was provided by the DOD-MURI program.

¹P. Hohenberg and W. Kohn, Phys. Rev. **136**, B864 (1964).

²E. Smargiassi and P. A. Madden, Phys. Rev. B **49**, 5220 (1994); **51**, 117

(1995); M. Foley, E. Smargiassi, and P. A. Madden, J. Phys.: Condens. Matter **6**, 5231 (1994); M. Foley, D. Phil. Thesis, Oxford University, UK, 1995; M. Foley and P. A. Madden, Phys. Rev. B **53**, 10589 (1996); B. J. Jesson, M. Foley, and P. A. Madden, *ibid.* **55**, 4941 (1997); J. A. Anta, B. J. Jesson, and P. A. Madden, *ibid.* **58**, 6124 (1998).

³Q. Wang, M. D. Glossman, M. P. Iñiguez, and J. A. Alonso, Philos. Mag. B **69**, 1045 (1993); S. C. Watson, D. Phil. Thesis, Oxford University, UK, 1996; S. C. Watson and P. A. Madden, PhysChemComm **1**, 1 (1998); S. C. Watson and E. A. Carter, Comput. Phys. Commun. **128**, 67 (2000).

⁴N. Govind, J. Wang, and H. Guo, Phys. Rev. B **50**, 11175 (1994); N. Govind, J. L. Mozos, and H. Guo, *ibid.* **51**, 7101 (1995); D. Nehete, V. Shah, and D. G. Kanhere, *ibid.* **53**, 2126 (1996); V. Shah, D. Nehete, and D. G. Kanhere, J. Phys.: Condens. Matter **6**, 10 773 (1994); V. Shah and D. G. Kanhere, *ibid.* **8**, L253 (1996); V. Shah, D. G. Kanhere, C. Majumder, and D. G. Das, *ibid.* **9**, 2165 (1997); P. Blaise, S. A. Blundell, and C. Guet, Phys. Rev. B **55**, 15856 (1997); A. Vichare and D. G. Kanhere, J. Phys.: Condens. Matter **10**, 3309 (1998); A. Aguado, J. M. López, J. A. Alonso, and M. J. Stott, J. Chem. Phys. **111**, 6026 (1999); J. Phys. Chem. **105**, 2386 (2001).

⁵D. R. Hartree, Proc. Cambridge Philos. Soc. **24**, 89 (1928); V. Fock, Z. Phys. **61**, 126 (1930); C. C. J. Roothaan, Rev. Mod. Phys. **23**, 69 (1951).

⁶W. Kohn and L. J. Sham, Phys. Rev. **140**, A1133 (1965).

⁷Y. A. Wang and E. A. Carter, *Theoretical Methods in Condensed Phase Chemistry* (Kluwer, Dordrecht, 2000), Chap. 5, pp. 117–184.

⁸L. H. Thomas, Proc. Cambridge Philos. Soc. **23**, 542 (1927); E. Fermi, Rend. Accad. Naz. Lincei **6**, 602 (1927); Z. Phys. **48**, 73 (1928).

⁹W. C. Topp and J. J. Hopfield, Phys. Rev. B **7**, 1295 (1973); J. A. Appelbaum and D. R. Hamann, *ibid.* **8**, 1777 (1973); M. Schlüter, J. R. Chelikowsky, S. G. Louie, and M. L. Cohen, *ibid.* **12**, 4200 (1975); Th. Starkloff and J. D. Joannopoulos, *ibid.* **16**, 5212 (1977); J. Ihm and M. L. Cohen, Solid State Commun. **29**, 711 (1979); L. Goodwin, R. J. Needs, and V. Heine, J. Phys.: Condens. Matter **2**, 351 (1990); F. Nogueira, C. Fiolhais, J. He, J. P. Perdew, and A. Rubio, *ibid.* **8**, 287 (1996); S. Watson, B. J. Jesson, E. A. Carter, and P. A. Madden, Europhys. Lett. **41**, 37 (1998); D. J. González, L. E. González, J. M. López, and M. J. Stott, Phys. Rev. B **65**, 184201 (2002); B. Wang and M. J. Stott, *ibid.* **68**, 195102 (2003).

¹⁰D. R. Hamann, M. Schlüter, and C. Chiang, Phys. Rev. Lett. **43**, 1494 (1979); U. von Barth and C. D. Gelatt, Phys. Rev. B **21**, 2222 (1980); G. B. Bachelet, D. R. Hamann, and M. Schlüter, *ibid.* **26**, 4199 (1982); G. P. Kerker, J. Phys. C **13**, L189 (1980); L. Kleinman and D. M. Bylander, Phys. Rev. Lett. **48**, 1425 (1982); D. Vanderbilt, Phys. Rev. B **32**, 8412 (1985); D. R. Hamann, *ibid.* **40**, 2980 (1989); A. M. Rappe, K. M. Rabe, E. Kaxiras, and J. D. Joannopoulos, *ibid.* **41**, 1227 (1990); D. M. Bylander and L. Kleinman, *ibid.* **41**, 907 (1990); X. Gonze, P. Käckell, and M. Scheffler, *ibid.* **41**, 12 264 (1990); M. Teter, *ibid.* **48**, 5031 (1993); N. J. Ramer and A. M. Rappe, *ibid.* **59**, 12 471 (1999); I. Grinberg, N. J. Ramer, and A. M. Rappe, *ibid.* **63**, 201102 (2001).

¹¹N. Troullier and J. L. Martins, Phys. Rev. B **43**, 1993 (1991).

¹²B. Zhou, Y. A. Wang, and E. A. Carter, Phys. Rev. B **69**, 125109 (2004).

¹³P.-O. Löwdin, Phys. Rev. **97**, 1474 (1955); R. McWeeny, Rev. Mod. Phys. **32**, 335 (1960); B. C. Carlson and J. M. Keller, Phys. Rev. **121**, 659 (1961); A. J. Coleman, Rev. Mod. Phys. **35**, 668 (1963); E. R. Davidson, *Reduced Density Matrices in Quantum Chemistry* (Academic, New York, 1976).

¹⁴R. G. Parr and W. Yang, *Density-Functional Theory of Atoms and Molecules* (Oxford University Press, New York, 1989); R. M. Dreizler and E. K. U. Gross, *Density Functional Theory: An Approach to the Quantum Many-Body Problem* (Springer, Berlin, 1990).

¹⁵M. Berrondo and O. Goscinski, Int. J. Quantum Chem., Symp. **9**, 67 (1975); P. D. Haynes and M. C. Payne, Solid State Commun. **108**, 737 (1998).

¹⁶W. Yang, Phys. Rev. A **34**, 4575 (1986).

¹⁷N. W. Ashcroft and N. D. Mermin, *Solid State Physics* (Saunders, Orlando, 1976); W. A. Harrison, *Solid State Theory* (Dover, New York, 1980); K. S. Singwi and M. P. Tosi, Solid State Commun. **36**, 177 (1981); J. Hafner, *From Hamiltonians to Phase Diagrams: the Electronic and Statistical-Mechanical Theory of sp-Bonded Metals and Alloys* (Springer, Berlin, 1987); D. Pines and P. Nozières, *The Theory of Quantum Liquids* (Addison-Wesley, New York, 1989) Vol. 1; D. G. Pettifor, *Bonding and Structures of Molecules and Solids* (Clarendon, Oxford, 1995).

- ¹⁸J. Lindhard, K. Dan. Vidensk. Selsk. Mat. Fys. Medd. **28**, 8 (1954).
- ¹⁹Y. Tal and R. F. W. Bader, Int. J. Quantum Chem., Symp. **12**, 153 (1978); P. K. Chattaraj and B. M. Deb, J. Sci. Ind. Res. **43**, 238 (1984).
- ²⁰J. M. C. Scott, Philos. Mag., Suppl. **43**, 859 (1952); P. A. M. Dirac, Proc. Cambridge Philos. Soc. **26**, 376 (1930); N. H. March, Adv. Phys. **6**, 1 (1957).
- ²¹C. F. von Weizsäcker, Z. Phys. **96**, 431 (1935).
- ²²J. Goodisman, Phys. Rev. A **1**, 1574 (1970); P. K. Acharya, L. J. Bartolotti, S. B. Sears, and R. G. Parr, Proc. Natl. Acad. Sci. U.S.A. **77**, 6978 (1980); J. L. Gázquez and J. Robles, J. Chem. Phys. **76**, 1467 (1982).
- ²³D. A. Kirzhnits, Sov. Phys. JETP **5**, 64 (1957); C. H. Hodges, Can. J. Phys. **51**, 1428 (1973); B. K. Jennings, R. K. Bhaduri, and M. Brack, Nucl. Phys. A **253**, 29 (1975); B. Grammaticos and A. Voros, Ann. Phys. (N.Y.) **123**, 359 (1979); D. R. Murphy, Phys. Rev. A **24**, 1682 (1981).
- ²⁴K. Yonei and Y. Tomishima, J. Phys. Soc. Jpn. **20**, 1051 (1965); Y. Tomishima and K. Yonei, *ibid.* **21**, 142 (1966); E. K. U. Gross and R. M. Dreizler, Phys. Rev. A **20**, 1798 (1979); W. Stich, E. K. U. Gross, P. Malzacher, and R. M. Dreizler, Z. Phys. A **309**, 5 (1982).
- ²⁵A. E. DePristo and J. D. Kress, Phys. Rev. A **35**, 438 (1987); G. I. Plindov and S. K. Pogrebnya, Chem. Phys. Lett. **143**, 535 (1988); H. Ou-Yang and M. Levy, Int. J. Quantum Chem. **40**, 379 (1991); H. Lee, C. Lee, and R. G. Parr, Phys. Rev. A **44**, 768 (1991); D. J. Lacks and R. G. Gordon, J. Chem. Phys. **100**, 4446 (1994).
- ²⁶J. A. Alonso and L. A. Girifalco, Phys. Rev. B **17**, 3735 (1978); M. D. Glossman, A. Rubio, L. C. Balbás, and J. A. Alonso, Int. J. Quantum Chem., Symp. **26**, 347 (1992); M. D. Glossman, A. Rubio, L. C. Balbás, J. A. Alonso, and Ll. Serra, Int. J. Quantum Chem. **45**, 333 (1993); M. D. Glossman, A. Rubio, L. C. Balbás, and J. A. Alonso, Phys. Rev. A **47**, 1804 (1993); Int. J. Quantum Chem., **49**, 171 (1994).
- ²⁷E. Chacón, J. E. Alvarellos, and P. Tarazona, Phys. Rev. B **32**, 7868 (1985); P. García-González, J. E. Alvarellos, and E. Chacón, *ibid.* **53**, 9509 (1996); Phys. Rev. A **54**, 1897 (1996); Phys. Rev. B **57**, 4857 (1998); Phys. Rev. A **57**, 4192 (1998).
- ²⁸L.-W. Wang and M. P. Teter, Phys. Rev. B **45**, 13 196 (1992).
- ²⁹M. Pearson, E. Smargiassi, and P. A. Madden, J. Phys.: Condens. Matter **5**, 3321 (1993); F. Perrot, *ibid.* **6**, 431 (1994).
- ³⁰Y. A. Wang, N. Govind, and E. A. Carter, Phys. Rev. B **58**, 13 465(E) (1998); *ibid.* **64**, 129901 (2001).
- ³¹Y. A. Wang, N. Govind, and E. A. Carter, Phys. Rev. B **60**, 16 350(E) (1999); *ibid.* **64**, 089903 (2001).
- ³²W. H. Press, S. A. Teukolsky, W. T. Vetterling, and B. P. Flannery, *Numerical Recipes in Fortran* (Cambridge University Press, Cambridge, 1992).
- ³³Y. A. Wang, Phys. Rev. A **55**, 4589 (1997).
- ³⁴K. M. Carling and E. A. Carter, Modell. Simul. Mater. Sci. Eng. **11**, 339 (2003).
- ³⁵D. M. Ceperley and B. J. Alder, Phys. Rev. Lett. **45**, 566 (1980); J. P. Perdew and A. Zunger, Phys. Rev. B **23**, 5048 (1981).
- ³⁶A. García, C. Elsässer, J. Zhu, S. G. Louie, and M. L. Cohen, Phys. Rev. B **46**, 9829 (1992); Y. Juan and E. Kaxiras, *ibid.* **48**, 14 944 (1993).
- ³⁷M. C. Payne, M. P. Teter, D. C. Allan, T. A. Arias, and J. D. Joannopoulos, Rev. Mod. Phys. **64**, 1045 (1992); M. D. Segall, P. J. D. Lindan, M. J. Probert, C. J. Pickard, P. J. Hasnip, S. J. Clark, and M. C. Payne, J. Phys.: Condens. Matter **14**, 2717 (2002); M. D. Segall, C. J. Pickard, R. Shah, and M. C. Payne, Mol. Phys. **89**, 571 (1996).
- ³⁸M. T. Yin and M. L. Cohen, Phys. Rev. B **26**, 5668 (1982).
- ³⁹J. Donohue, *The Structure of the Elements* (Wiley, New York, 1974).
- ⁴⁰H. J. Monkhorst and J. D. Pack, Phys. Rev. B **13**, 5188 (1976).
- ⁴¹F. D. Murnaghan, Proc. Natl. Acad. Sci. U.S.A. **30**, 244 (1944).